Reward Systems and Food Avoidance in Adolescents with Low Weight Eating Disorders

PI: Tom Hildebrandt

NCT02795455

Document Date: 4/12/2022

Statistical Analysis

Due to the 7-year difference of when the grant was written and completion of the project, the analytic plan for the project has evolved. To meet the evolving ClinicalTrials.gov standards of transparency, an excerpt of the approved grant application containing the original statistical analysis plan has been provided in this document. However, please reference published papers for applied approaches. Generally, the investigators will conduct conditional longitudinal data models (ANCOVA with random intercept), which adjusts time 2 endpoints on baseline differences accounting for random intercept, with our primary outcomes the mean difference between treatments at time 2.

Grant Excerpt:

D.1 PREPARATION OF fMRI-EMG DATA

D.1.1 Preprocessing of functional images. Functional time series for the reversal learning task acquired at baseline for all subjects will be individually slice-time corrected, motion corrected, co-registered to the T2 structural volume, normalized to the Montreal Neurological Institute template, and spatially smoothed with a 6- mm FWHM Gaussian kernel. The functional time series acquired at the endpoint will be further co-registered to the baseline time series and the two time series will then be jointly normalized and smoothed.

D.1.2 First-level analysis: individual modeling of activation. Event-related analyses of activation will be conducted individually for each subject. General linear models (GLM) will be used to fit beta weights to regressors for the 4 trial events of interest (CS+ and CS- during acquisition and reversal) and as well as 3 trial events (response, UCS+, UCS-) and 6 motion parameters of no interest in the baseline and endpoint scans, convolved with the hemodynamic response function (HRF). Mean EMG amplitude for the levator labii superioris will be entered as a parametric modulator of CS+ events during acquisition (DAcquisition) and reversal (DReversal). *Mean EMG amplitude for zygmaticus activation will be entered as a parametric modulator of CS- events during reversal (PReversal).* The neural effects of food-cue acquisition, food-cue extinction, *and cued food absence* will be tested by applying linear contrasts to the beta weights for CS+ vs. fixation during acquisition, CS+ vs. fixation during reversal, *and CS- vs. fixation during reversal*, respectively, for both the baseline scan alone and the endpoint minus baseline scans. The modulation of these effects by disgust *and pleasure* will be tested by applying linear contrasts to the beta weights for DAcquisition, DReversal, and *PReversal*. *The baseline CS+Acquisition, CS+Reversal, and CS-Reversal contrast images for controls will be entered into one-sample t-tests to define 'normal' IAVS activation for food-cue acquisition and dlPFC and vmPFC activation for food-cue extinction and cued food absence*. *The results will inform the connectivity analyses.*

D.1.3 First-level analysis: individual modeling of psychophysiological interaction (PPI). PPI will be conducted twice using 1) the baseline contrasts to test the whole-brain functional connectivity of IAVS and prefrontal regions of interest (ROI) for food-cue acquisition and extinction and *cued food absence* and 2) the endpoint minus baseline contrasts to test the effect of the interventions *(*or time in controls*)* on this connectivity. The seed ROI shown in **Figure 4** will be defined as a 6-mm radius sphere at subject-specific maxima that are within 4 mm of the 'normal' coordinates defined in the previous section and restricted to the same anatomical area using the automated anatomical labeling template. Regressors representing the neuronal time series (Y regressor), the CS+Acquisition, CS+Reversal, *CS-Reversal,* DAcquisition, DReversal, or PReversal contrasts (P regressor), and the interaction between physiological and psychological factors (PPI regressor) will be forward-convolved with the HRF and then entered into subject-specific GLMs, along with six motion parameters of no interest. Functional connectivity for food-cue acquisition, food-cue extinction, and cued food absence*,* and the effect of the interventions *(or time for controls)* on this connectivity will be tested by applying linear contrasts to the beta weights for the baseline and endpoint minus baseline PPI regressors. The resultant contrast images will be used to test for group differences in baseline connectivity/disgust modulation (hypotheses 1a-c and 2a-d) and differences in the effects of the interventions on this connectivity (hypotheses 3a-d and 4a-b). **D.1.4 First-level analysis: individual dynamic causal modeling (DCM).** DCM will be conducted twice using 1) the baseline contrasts to infer the directionality of the IAVS-prefrontal connectivity for food-cue acquisition, food-cue extinction, and cued food absence and 2) the endpoint minus baseline contrasts to infer the

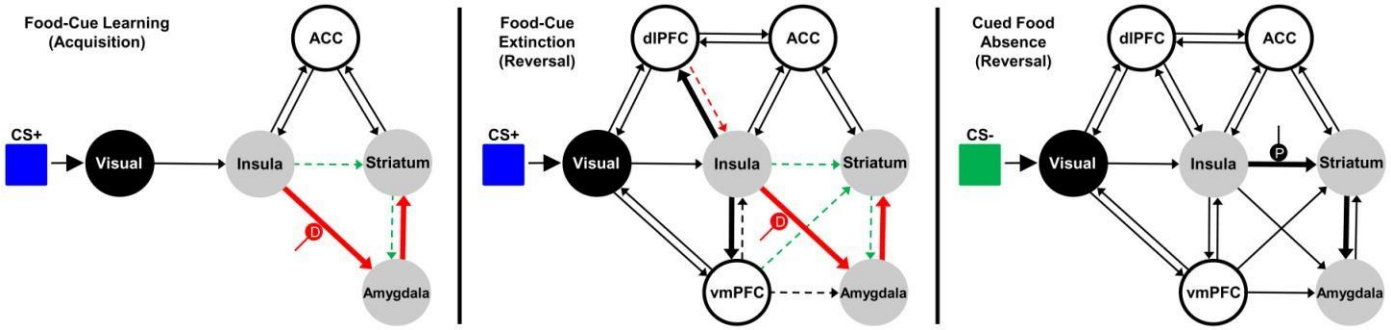

Figure 4. Hypothesized models of the effective connectivity of food-cue learning and extinction and cued food absence. Black, gray, and white circles denote sensory, saliency, and regulatory nodes, respectively. Thick lines and dashed lines denote stronger and weaker connectivity, respectively, in LW-EDs compared to controls. Circular markers indicate modulation by EMG measures of disgust (D) and pleasure (P) in LW-EDs but not controls. Hypothesized sites of therapeutic actions of IE and FBT-WG are shown in red and green, respectively.

directionality of the effects of intervention *(*or time in controls*)* on IAVS-prefrontal connectivity. The three *a priori* DCMs shown in **Figure 4** will be specified individually for all subjects using the ROI defined in the prior section. The main effects of CS+Acquisition, CS+Reversal, *and* CS-Reversal will be entered as driving inputs to the visual cortex during food-cue acquisition, food-cue extinction, and cued food absence, respectively. DAcquisition and DReversal will be entered as modulators of insula amygdala connectivity *and PReversal* as a modulator of insula striatum connectivity for the LW-EDs group only. The *a priori* models will be elaborated into alternative models that systematically vary: i) the directionality of each functional connection between the nodes; and ii) the modulation of each of these connections by the EMGs measure of disgust and pleasure (LW-EDs only).

The *a priori* models of food-cue acquisition, food-cue extinction, and cued food absence will be compared to the alternative models separately in LW-EDs and controls using a series of random-effects Bayesian model selection (BMS)174-176 to compute exceedance and posterior probabilities at the group level. Families of models defined by shared features will initially be tested in order to focus on individual models that best fit the data.

The exceedance probability will be used to identify the models with the greatest supporting evidence in each group given the observed fMRI data. Random-effects Bayesian model averaging (BMA)177 will be used to obtain average connectivity estimates for the IAVS-prefrontal interactions of interest, and these connectivity estimates will be used to test for group differences in baseline connectivity/ modulation (hypotheses 1a-c and 2a-d). These procedures will be repeated using the endpoint minus baseline contrasts to create DCMs for food-cue acquisition and extinction separately for controls and adolescents with LW-EDs treated with IE and FB-WG. BMA connectivity estimates for the IAVS-prefrontal interactions of interest will be used to test for differences in the effects of the interventions on IAVS-prefrontal connectivity in hypotheses *3a-d and 4a-b*.

D.2 HYPOTHESIS TESTING

The hypotheses will each be tested with a series of random-effects GLM that will use one-way analyses of covariance (ANCOVA), in which the PPI contrast images section and BMA connectivity estimates described above will serve as the dependent measures of IAVS-prefrontal connectivity and Group (either LW-EDs vs. Controls or IE vs. FB-WGC vs. Controls) as a between-subject factor. Age will be entered as a covariate. Statistical significance will be adjusted for the number of tests of each hypothesis (e.g., $p = 0.05 / 2$ tests $= 0.025$) and will be corrected for multiple voxel comparisons using the false discovery rate (FDR) method.

D.2.1 Hypothesis 1 (a) The insula-driven activation of amygdala and amygdala→striatum connectivity for food-cue acquisition (i.e., CS+ or anticipated food reward) will be enhanced in LW-EDs compared to controls. The PPI contrast images for insula, amygdala, and striatum and the BMA estimates for insula→amygdala and amygdala→striatum connectivity for the baseline $CS+_{Acquisition}$ contrast will be entered into separate ANCOVAs with significance set at $p < 0.01$. The hypothesis would be supported by findings of

significantly greater insula→amygdala and amygdala→ striatum connectivity in LW-EDs than controls. **(b) The insula-driven activation of amygdala will be moderated by the disgust response in LW-EDs but not controls.** The PPI contrast image for insula and BMA estimate for insula→amygdala connectivity for the $D_{Acquisition}$ contrast will be tested using separate ANCOVA with significance set at $p < 0.025$. The hypothesis would be supported by findings of disgust modulation of insula→amygdala connectivity in LW-EDs that is absent or significantly lower in controls. **(c) The reduced incentive value of food will be reflected in weaker insula-driven activation of ventral striatum and striatum→amygdala connectivity in LW-EDs compared to controls.** The BMA estimates for insula→striatum and striatum→amygdala connectivity for the baseline $CS+_{Acquisition}$ contrast will be entered into separate ANCOVAs with significance set at $p < 0.025$. The insulastriatum-amygdala functional connectivity will be tested for hypothesis 1a. The hypothesis would be supported by findings of lower insula→striatum and striatum→amygdala effective connectivity in LW-EDs than controls.

D.2.2 Hypothesis 2 (a) The disgust-driven insula→amygdala and amygdala→striatum connectivity for food-cue reversal (i.e., CS+ or no food reward) will be enhanced in LW-EDs compared to controls. The procedures described in section D.2.1a above will be used to confirm the group differences in the same 5 PPI contrast images and BMA estimates for the baseline $CS+_{Reversal}$ contrast. **(b) Enhanced 'bottom-up' insula-driven activation of dlPFC and vmPFC in LW-EDs compared to controls.** The PPI contrast images for dlPFC and vmPFC and the BMA estimates for insula→dlPFC and insula→vmPFC connectivity for the baseline $CS+_{Reversal}$ will be entered into separate ANCOVAs with significance set at $p < 0.0125$. The hypothesis would be supported by findings of greater insula→dlPFC and insula→vmPFC connectivity in LW-EDs than controls. **(c) Weaker 'top-down' dlPFC and vmPFC control of insula, amygdala, and striatum in LW-Eds compared to controls.** The BMA estimates for dlPFC→insula and vmPFC→insula connectivity for the baseline $CS+_{Reversal}$ contrast will be entered into separate ANCOVAs with significance set at $p < 0.025$. The functional connectivity of insula with dlPFC and vmPFC will be tested for hypothesis 2b. The hypothesis would be confirmed by findings of less dlPFC→ insula and vmPFC→insula connectivity in LW-EDs than controls. **(d) The insula-driven activation of ventral striatum for the cued-absence of food will be moderated by the pleasure response in LW-EDs but not controls.** The PPI contrast image and BMA estimate for the $P_{Reversal}$ contrast will be tested using separate ANCOVA with significance set at $p < 0.025$. The hypothesis would be supported by findings of pleasure modulation of insula→striatum connectivity in LW-EDs but not controls.

D.2.3 Hypothesis 3 (a) Treatment with IE will diminish disgust-driven insula activation of amygdala and amygdala→striatum connectivity for food-cue acquisition. The procedures described in sections D.2.1.a and D.2.1.b will be used with the endpoint minus baseline $CS+_{Acquisition}$ and $D_{Acquisition}$ contrasts to compare the effects of IE treatment to FB-WGC treatment and untreated controls. Significance will be set at $p <0.008$ for the 6 tests. The hypothesis would be supported by findings of significantly greater reductions in both insula→amygdala and amygdala→striatum connectivity and disgust-modulation of this connectivity for IE treatment compared to FB-WGC treatment and untreated controls. **(b) IE treatment will strengthen 'topdown' dlPFC control of insula for food-cue reversal.** The PPI contrast image for dlPFC and BMA estimate for dlPFC→insula connectivity for the endpoint minus baseline $CS+_{Reversal}$ contrast will be entered into separate ANCOVAs with significance set at $p < 0.025$. The hypothesis would be supported by findings of significantly greater increases in dlPFC→insula connectivity for IE treatment compared to FB-WGC treatment and untreated controls. **(c) Treatment with FB-WG will strengthen incentive-driven insula activation of ventral striatum and striatum→amygdala connectivity for food-cue acquisition.** The procedures described in sections D.2.1.c will be used with the endpoint minus baseline $CS+_{Acquisition}$ contrast to compare the effects of FB-WG treatment to IE treatment and untreated controls. Significance will be set at $p <0.0125$ for the 4 tests. The hypothesis would be supported by findings of significantly greater increases in insula→ striatum and striatum→amygdala connectivity for FB-WGC treatment compared to IE treatment and uncontrolled controls. **(d) FB-WG treatment will increase 'top-down' vmPFC control of ventral striatum for food-cue reversal.** The PPI contrast image for dlPFC and BMA estimate for dlPFC→insula connectivity for the endpoint minus baseline $CS+_{Reversal}$ contrast will be entered into separate ANCOVAs with significance set at $p < 0.025$. The hypothesis would be supported by findings of significantly greater increases in vmPFC→ striatum connectivity for FB-WGC treatment compared to IE treatment and untreated controls.

D.2.4 Hypothesis 4 (a) Laboratory and real-world measures of Kcal consumed will correlate

negatively with insula-driven food-cue acquisition and positively with prefrontal-driven food-cue extinction at baseline across LW-EDs and control groups. The baseline PPI contrast images and BMA estimates for connections identified in sections D.2.1 and D.2.2 will be entered for all subjects into separate linear regression analyses with percent change in Kcal (i.e., baseline – endpoint / baseline) as the regressor and age as a covariate. Significance will be adjusted for the number of tests. This hypothesis would be supported by significant correlations of baseline Kcal with IAVS connectivity for food-cue acquisition and prefrontal connectivity for food-cue extinction. (**b**) **Δ in Kcal consumed on laboratory and real-world measures will correlate negatively with change in food-cue acquisition and positively with change in extinction for IE compared to FB-WG.** The endpoint minus baseline PPI contrast images and BMA estimates for connectivity identified in section D.2.3 will be entered into separate multiple regression analyses with three regressors: (i) intervention type (IE vs. FB-WG); (ii) percent change in Kcal (i.e., baseline – endpoint / baseline); and (iii) an interaction predictor. The regressors will be de-meaned and the interaction term will be calculated as the product of the de-meaned regressors. Statistical significance will be set at the relatively liberal level of $p < 0.05$ corrected using FDR. This hypothesis will be supported by findings of significant changes in IAVS-prefrontal connectivity associated with the interaction term, such that the Kcal change score correlates with different IAVS connectivity for food-cue acquisition and prefrontal connectivity for extinction in adolescents treated with IE compared to those treated with FB-WG.

D.3 Statistical Power Considerations: Power considerations are primarily related to the need to detect the differential increases/decreases in effective connectivity hypothesized in Aim-III. The effect sizes were taken from pilot (**C.7**) and our published data[21,50,86,104]. Results indicate that a sample of N=90, 30 per group, will achieve a power of 0.88-0.94 to within-subject changes in connectivity. We powered our study for moderate between group ANCOVA effects (R_2 =0.30) **D.2.1-3.** Using Monte Carlo simulation (10,000 draws), we recovered moderate effects from 84% to 92% of draws depending on ANCOVA model, and with 15% attrition we recovered hypothesized effects on 77% to 92% of draws. We estimated age covariate effects at r =.15 based on pilot data. Thus, we should have sufficient power to detect medium sized effects of IE and FBT-WG. Power for **D.2.4**. used estimated effects from Dr. Sysko's work with adult AN and eating behavior[49,52,148]. Although we didn't conduct formal power analysis of DCM, our sample size is consistent with published power recommendations for this methodology[178]. We will use all available data and conduct sensitivity analysis for missing data[179] (i.e., dropout, attrition) using MAR vs. completer models built for fMRI modeling.